Targeting α7 Nicotinic Acetylcholine Receptor for Modulating the Neuroinflammation of Dry Eye Disease Via Macrophages

Xujiao Zhou,[1,2] Yuqing Wu,[1] Yirou Zhang,[1] Binbin Chu,[3] Kan Yang,[4] Jiaxu Hong,[1,2,5–8] and Yao He[9,10]

[1]Department of Ophthalmology, Eye and ENT Hospital, Fudan University, Shanghai, China
[2]Shanghai Key Laboratory of Gene Editing and Cell Therapy for Rare Diseases, Fudan University, Shanghai, China
[3]Institute of Functional Nano and Soft Materials Soochow University, Suzhou, China
[4]Department of Ophthalmology, The First People's Hospital of Lanzhou City, Gansu, China
[5]Department of Ophthalmology, Eye & ENT Hospital, State Key Laboratory of Medical Neurobiology and MOE Frontiers Center for Brain Science, Fudan University, Shanghai, China
[6]NHC Key laboratory of Myopia and Related Eye Diseases Shanghai, China
[7]Shanghai Key Laboratory of Rare Disease Gene Editing and Cell Therapy; Shanghai Engineering Research Center of Synthetic Immunology, Shanghai, China
[8]Department of Ophthalmology, Children's Hospital of Fudan University, National Pediatric Medical Center of China, Shanghai, China
[9]Macao Translational Medicine Center, Macau University of Science and Technology, Taipa, China
[10]Institute of Materials Science and Engineering, Macau University of Science and Technology, Taipa, China

Correspondence: Xujiao Zhou, EENT, Fudan University, No. 83 Fenyang Rd., Shanghai 200031, China; xujiao.zhou@fdeent.org.
Yao He, Macau University of Science and Technology, Taipa Rd., Macau 999078, China; yaohe@must.edu.mo.
Jiaxu Hong, EENT, Fudan University, 83 Fenyang, Shanghai 200031, China; Jiaxu.hong@fdeent.org.

XZ, YW, YZ, and BC contributed equally to this study.

Received: January 25, 2025
Accepted: April 10, 2025
Published: May 6, 2025

Citation: Zhou X, Wu Y, Zhang Y, et al. Targeting α7 nicotinic acetylcholine receptor for modulating the neuroinflammation of dry eye disease via macrophages. *Invest Ophthalmol Vis Sci.* 2025;66(5):13. https://doi.org/10.1167/iovs.66.5.13

Purpose. Patients with dry eye disease (DED) often exhibit neurological abnormalities and may even suffer from neuropathic pain and pain-related anxiety or depression. The α-7 nicotinic acetylcholine receptor (α7nAChR) is a pivotal regulator in the anti-inflammatory pathway connecting the nervous and immune systems, Here, we investigate the potential of α7nAChR agonist as a novel treatment for DED.

Methods. We induced DED model by unilateral excision of extraorbital lachrymal gland in C57/BL6 mice. After seven days of treatment, RNA sequencing was performed to identify differentially expressed genes in the cornea of lacrimal gland excision (LGE) mice. Quantitative polymerase chain reaction, Western blotting, and flow cytometry tests were carried out to elucidate neuroinflammation changes after α7nAChR activation. Corneal nerve abnormalities were assessed by corneal esthesiometry and immunofluorescence staining.

Results. The activation of α7nAChR stimulates genes involved in immune-mediated inflammatory progression and neuroregulation, inhibits the expression of transient receptor potential vanilloid-1, reinstates corneal nerve density, and alleviates anxiety-like behaviors associated with severe DED. Furthermore, we demonstrated that α7nAChR agonist restored corneal nerve abnormality and alleviated inflammation response by down-regulating the proportion of $CD86^+$ M1 macrophages (proinflammatory phenotypes).

Conclusions. Our findings underscore the activation of α7nAChR as a pioneering therapeutic approach for preserving corneal nerves balance and controlling inflammation in DED.

Keywords: dry eye disease, neuroinflammation, α7 nicotinic acetylcholine receptor, macrophages

Dry eye is a prevalent eye surface disease, with patients presenting complaints of eye dryness, itching, foreign body sensation, burning sensation, and fluctuating vision.[1] It is increasingly associated with excessive use of digital devices and escalating environmental pollution, particularly affecting younger individuals.[2–5] This trend has been observed to not only impact work efficiency but also diminish visual-related quality of life. The intricate development of dry eye is believed to stem from a cycle of interrelated factors, contributing significantly to its pathogenesis. The latest international consensus on dry eye (TFOS DEWS II) highlights the influential role of neuronal regulation abnormalities in the development of the condition.[6–9] Clinical assessment of dry eye using in vivo confocal microscopy has revealed corneal nerve abnormalities,[10] including reduced nerve density,[11] increased tortuosity,[11,12] as well as

diminished[13] or enhanced[14] sensation. Dry eye patients in clinical settings endure tormenting eye pain and long-term psychological stress from anxiety, which serves as a primary motivator for seeking medical care. However, unlike conventional anti-inflammatory and tear supplementation treatments, addressing dry eye nerve abnormalities presents a pressing need for targeted therapies in clinical practice yet is hindered by the lack of directly applicable medications.

Through the analysis of data from 648 dry eye patients, it was found that chronic pain over the long term can induce an elevation in the release of inflammatory mediators in the blood, consequently lowering the pain threshold and resulting in heightened pain sensitivity.[15] The corneal epithelium contains a significant number of trigeminal nerve endings,[13] with these nerve fiber endings exhibiting high expression of the transient receptor potential vanilloid 1 (TRPV1). TRPV1 signaling, as induced by transient hyperosmolarity, leads to neuroimmune abnormalities in a murine model of dry eye[16] and has also been directly linked to the propagation of corneal nerve damage,[17] which exacerbates dryness sensation and discomfort. SYL1001, a short interfering siRNA targeting the TRPV1, designed for the prevention and treatment of eye pain and dry eye syndrome, is currently undergoing two Phase II clinical trials (NCT01776658 and NCT02455999). A recent study compared the effects of topical administration of SYL1001 eye drops (once daily for 10 days) in 156 healthy individuals and dry eye patients.[18] However, although SYL1001 can alleviate eye pain, it does not halt disease progression, serving as a palliative rather than a curative measure. Direct attempts at inhibiting TRPV1 have faced challenges in clinical translation, with prior studies yielding unsuccessful results.[18]

Dysregulation of the immune system is a common complication in pain patients, suggesting an underlying connection between pain and immunity. Growing evidence indicates that neuro-inflammation and neuro-immune reactions play a critical role in the pathological progression of dry eye and chronic pain.[19] Corneal nerves regulate inflammation through neuro-immune interactions by secreting neurotransmitters,[20] including norepinephrine, neuropeptide Y (NPY), and calcitonin gene–related peptide released by the sympathetic nervous system,[21] as well as acetylcholine (ACh) released by the parasympathetic nervous system. Among these neurotransmitters, acetylcholine and its receptors have garnered increasing attention in the realm of neuro-immune interactions. The α7 nicotinic acetylcholine receptor (α7nAChR) is a key protein in the cholinergic anti-inflammatory pathway (CAP) that connects the nervous and immune systems.[22] Administering α7nAChR agonists locally can aid in hastening corneal wound healing and regulating inflammation.[23] Varenicline nasal spray has been approved by the U.S. Food and Drug Administration as the first and only nasal spray medication for treating both symptoms and signs of dry eye.[24,25] With its high affinity and selectivity, varenicline binds to human α3β4, α4β2, α3α5β4, α4α6β2, and α7nAChRs.[26] Furthermore, research has identified the early infiltration of $CD11b^+$ macrophages as a characteristic feature of corneal damage in dry eye.[27] The α7nAChR present on macrophages can inhibit the release of TNF-α in macrophages, thereby attenuating the inflammatory response.[22]

In this study, we successfully established a mouse model of dry eye with corneal nerve abnormalities by performing extraorbital lacrimal gland surgeries.[28] We investigated the effects of the specific α7nAChR receptor agonist, PNU-282987, administered topically, on restoring the epithelial barrier, enhancing nerve innervation, alleviating ocular surface inflammation through inhibition of M1-type macrophage polarization, and ultimately reducing anxiety-like behavior in dry eye mice.

Methods

Animals and Ethics

The C57BL/6J (six to eight weeks old; male) were kept under standard conditions (12-hour day/12-hour night cycle, standard suitable humidity and temperature) with free access to food and water. All tests were approved by the Eye, Otolaryngology Hospital Attached to Fudan University's Animal Ethics Committee in accordance with a statement made by the Association for Research in Vision and Ophthalmology (ARVO) (Number: IRBEENT-2021 0301b).

Dry Eye Models

The C57BL/6J (six to eight weeks old; male) were used for establishing lacrimal-gland-excision dry eye model. Mice were anesthetized by intraperitoneal injection of 1.25% Avertin (15ul/g). After disinfecting with povidone-iodine, a 5 mm incision was made forward to the ear, and the extraorbital lacrimal glands were visible and excised.[29] Then, the incision was sutured by 6–0 nylon thread.[30]

Drug and Treatment

Fourteen days after lacrimal gland excision, mice received bilateral administration of drugs. PNU-282987 is a selective α7 nicotinic acetylcholine receptor.[31] For preparation, 50 mg PNU (MCE, Cat no. HY-12560A) were dissolved in 16.60 mL PBS to get 10 mM PNU. For the gradient experiment, PNU (10 mM) was diluted sequentially with PBS to 2.0 mM, 1.0 mM, 0.5 mM, 0.2 mM, and 0.1 mM, with each mouse receiving 5 µL per eye, twice daily for seven consecutive days.

Based on our drug concentration screening results, we selected a concentration of 1 mM for PNU-282987 in subsequent experiments. For the treatment of lacrimal gland excision (LGE)-induced dry eye disease model, PNU-282987 was used at a concentration of 1 mM, with each mouse receiving 5 µL per eye, twice daily for seven consecutive days. Methyllycaconitine (MLA) is a selective α7nAChR antagonist.[31] For preparation, 10 mg MLA (MCE, Cat no. HY-N2332A) were dissolved in 11.43 mL DMSO to get 1 mM MLA. MLA (1 mM) 5 µL was injected into the subconjunctiva every other day for each eye.[32] Clodronate liposomes were purchase from YEASEN (Shanghai, China).[33,34] Clodronate liposomes consist of clodronate encapsulated within lipid vesicles. This formulation specifically targets phagocytic macrophages, which engulf and degrade the liposomes, leading to intracellular accumulation of clodronate, subsequent induction of cellular apoptosis and global depletion of macrophages.[35] Clodronate liposomes was thoroughly mixed and brought to room temperature before using. For each mouse, 5 µL of clodronate liposomes were administrated through subconjunctival injection every other day for each eye.

Investigative Ophthalmology & Visual Science

Corneal Fluorescein Sodium Staining Score

After staining with fluorescein sodium for 60 seconds, the corneal epithelium was evaluated by a microscope with a cobalt blue light. Every cornea was equally divided into four quadrants and scored separately. The final score was obtained by adding all the scores. Scoring criteria: 0 point, no staining; 1 point, less than 30 stained dots; 2 points, more than 30 non-diffuse stained dots; 3 points, with remarkable diffuse staining but no plaque staining; 4 points, with a patchy stain. Staining pictures were captured at seven days after administration.

Schirmer I Test

Schirmer I was tested with Zone-Quick Phenol-Red cotton thread (Yokota, Japan) at one week after treatment. The eyelid was gently opened after general anesthesia, and 1 mm of the thread was put into lower eyelid conjunctiva near the canthus for 15 seconds. The length of phenol-red part was measured to represent tear production capacity. After the test was completed, the eyelids were closed to avoid overexposure.

Corneal Sensation

The Cochet–Bonnet aesthesiometer (Luneau, France) was used to quantitatively measure corneal sensation. Measurement began with the filament extended to its maximal length of 60 mm and shortened in 5-mm fractions until the corneal touch threshold was found. The center of the cornea was tested four times with each length, and a positive response was considered when the animal blinked more than or equal to 50% the number of times tested.[36] The longest filament length at which the animal felt the filament was recorded.

Cell

RAW 264.7 cells (Procell Life Science & Technology) were cultured in DMEM growth medium supplemented with 10% FBS and 1% penicillin/streptomycin at 37°C in a humidified 5% CO_2 atmosphere. Cells were pretreated for 30 minutes in the absence or presence of 5 µM MLA before adding 100 µM PNU282987. About two hours later, cells were induced with 1 µg/mL LPS (Sigma-Aldrich Corp., St. Louis, MO, USA) for 12 hours. Untreated RAW264.7 macrophages were used as a control. The dosages of these reagents were optimized according to previous experiments.[37]

Flow Cytometry

Preparation of single-cell suspension from cornea and conjunctiva in mice. The tissues were then cut into pieces and digested in RPMI 1640 medium with 1 mg/mL collagenase type IV (Cat no. 10608ES25; Yeasen Biotechnology, Shanghai, China) and 0.5 mg/mL DNase I (Cat no. 10608ES25; Yeasen) for 15 minutes at 37°C.[38,39] Then, cells were filtered separately through a 70-µm cell strainer.

For preparation of single-cell suspension, RAW264.7 cells are detached from the culture plate using a pipette and filtered separately through a 70-µm cell strainer. After the preparation of single-cell suspension, cells were blocked by anti-mouse CD16/CD32 (Cat no. 553141; BD Bioscience, Franklin Lakes, NJ, USA) for 30 minute and stained with nicotinic acetylcholine receptor alpha 7/CHRNA7 (Cat no. sc-58607; Santa Cruz Biotechnology, Dallas, TX, USA). Cells then treated with anti-CD45 Alexa Fluor F700 (Cat no. 103128; BioLegend, San Diego, CA, USA), anti-CD11b PE (Cat no. 101207; BioLegend), anti-F4/80 APC (Cat no. 101205; BioLegend), anti-CD86 Brilliant Violet 421 (Cat no. 105123; BioLegend), and FITC conjugated anti-Rat IgG (Cat no. SA00003-11; Proteintech, Rosemont, IL, USA) secondary antibody, and analyzed by a BD FACSCelesta (BD Bioscience) flow cytometer.

Quantitative Polymerase Chain Reaction (qPCR)

RNA of corneal tissue was extracted with Universal RNA Purification Kit (EZBioscience, Roseville, MN, USA) and was converted into first-strand complementary DNA using Color Reverse Transcription Kit (EZBioscience) according to the manufacturer's instructions. Quantitative PCR experiments were performed with 2 × Color SYBR Green qPCR Master Mix (EZBioscience) and QuantStudio 3 Real-Time PCR Systems (Thermo Fisher Scientific, Waltham, MA, USA). Cycle threshold (CT) means the number of cycles required for the fluorescent signal to exceed a threshold. Lower CT values indicate higher expression levels. Actin was used as a reference gene. Expression was calculated by relative quantification using the $2^{-\Delta\Delta CT}$ method. To normalize the target gene expression by calculating the difference in CT values (ΔCT) between the target gene and the reference gene. ΔΔCT: The difference in ΔCT values between a treated sample and a control sample (sham group). The primers used in this study were as follows: *m-Actin*-F: GGCTGTATTCCCCTCCATCG; m-*Actin*-R: CCAGTTGGTAACAATGCCATGT; m-*Il-6*-F: CTGCAAGAGACTTCCATCCAG; m-*Il-6*-R: AGTGGTATAGACAGGTCTGTTGG; m-*Il-1β*-F: AGCTTCAGGCAGGCAGTATC; m-*Il-1β*-R: AAGGTCCACGGGAAAGACAC; m-*Tnf-α*-F: CTGAACTTCGGGGTGATCGG; m-*Tnf-α*-R: GGCTTGTCACTCGAATTTTGAGA; m-*Mmp9*-F: CTGGACAGCCAGACACTAAAG; m-*Mmp9*-R: CTCGCGGCAAGTCTTCAGAG; m-*Adgre1*-F: CATAATCGCTGCTGGTTGAA; m-*Adgre1*-R:GATGAAAATCTGGGCAATGG; m-*Ccr7*-F: TGTACGAGTCGGTGTGCTTC; m-*Ccr7*-R: GGTAGGTATCCGTCATGGTCTTG; m-*Npy*-F: ATGCTAGGTAACAAGCGAATGG; m-*Npy*-R, TGTCGCAGAGCGGAGTAGTAT.

Western Blotting

Corneal protein was extracted using radioimmunoprecipitation assay lysis buffer (Solarbio, Beijing, China) sonicated on ice. The tissue lysates were spun in a centrifuge at 12,000*g* for 10 minutes at 4°C. The supernatants were separated for further analysis. Protein content was determined by bicinchoninic acid protein assay (P0010; Beyotime Biotechnology, Shanghai, China). Quantified amounts of total corneal protein were loaded per lane onto 10% SDS-PAGE and transferred onto polyvinylidene difluoride membrane. The membranes were blocked and then incubated with primary antibodies against rabbit anti-Actin (1:5000, ab179467; Abcam, Cambridge, MA, USA), anti-CD11b (1:1000, ab184308-40ul; Abcam), anti-TRPV1 (1:1000, ab305299-10ul; Abcam) overnight at 4°C. The membranes were then washed and incubated with HSP-conjugated anti-rabbit IgG (1:20,000, Cat no. 12-348; Merck, Kenilworth, NJ, USA) secondary antibodies for one hour at room temperature. Blots were washed and developed with a chemiluminescent reagent. The signals were visualized with a Kodak imaging system (Kodak, Rochester, NY, USA) and quali-

fied with ImageJ software (NIH, Bethesda, MD, USA). The uncropped images in Figure 2F are shown in Supplementary Figure S4. To normalize, select the results of Sham group as control and calculate the mean value of Sham group. The normalized value for each data point = (Experimental Value)/(Control Mean). Use the normalized values for further statistical analysis and comparisons.

RNA-Seq Database Construction Sequencing and Bioinformatics Analysis

Corneal RNA was extracted and quality of RNA samples was strictly controlled. RNA integrity and DNA contamination were assessed via agarose gel electrophoresis. Nanodrop was used for RNA concentration and purity detection. The Agilent 2100 BioAnalyzer (Agilent, Santa Clara, CA, USA) accurately detects RNA integrity. Ribosomal RNA was eliminated from total RNA, which was then broken into short fragments of 250–300 bp. The first complementary DNA (cDNA) strand was synthesized using the fragment RNA as the template and random oligonucleotide as the primer. Rnase H degraded the RNA strand. The second strand of cDNA was synthesized from deoxyribonucleotide triphosphates (dNTPs) under the DNA polymerase I system. The purified double-stranded cDNA underwent end repair and addition of "A" tails before sequencing. AMPure XP beads (Beckman Coulter, Inc, Southfield, MI, USA) were used to screen 350–400 bp of cDNA. The second strand of cDNA containing U was degraded by USER enzyme, and PCR amplification was performed to obtain the library.

RNA Sequencing and Differentially Expressed Genes Analysis

The libraries were sequenced on an llumina Novaseq 6000 platform (Illumina, San Diego, CA, USA) and 150 bp paired-end reads were generated. Raw reads of fastq format were firstly processed using fastp,[40] and the low-quality reads were removed to obtain the clean reads. The clean reads were mapped to the reference genome using HISAT2.[41] FPKM[42] of each gene was calculated and the read counts of each gene were obtained by HTSeq-count.[43] PCA analysis were performed using R (v3.2.0) to evaluate the biological duplication of samples.

Differential expression analysis was performed using the DESeq2.[44] P value < 0.05 and fold change >2 or <0.5 was set as the threshold for significantly differential expression gene (DEGs). Hierarchical cluster analysis of DEGs was performed using R (v3.2.0) to demonstrate the expression pattern of genes in different groups and samples. The radar map of top 30 genes was drawn to show the expression of up-regulated or down-regulated DEGs using R packet ggradar. Based on the hypergeometric distribution, GO[45], KEGG pathway,[46] Reactome, and WikiPathways enrichment analysis of DEGs were performed to screen the significant enriched term using R (v3.2.0), respectively. R (v3.2.0) was used to draw the column diagram, the chord diagram and bubble diagram of the significant enrichment term.

Immunofluorescence Staining for Corneal Flat Mounts

The cornea flat mounts were fixed in 4% paraformaldehyde for one hour, permeabilized with 20 mM/l EDTA for 1.5 hours, and then blocked with 10% Triton X-100/5% BSA for two hours at room temperature. The samples were incubated with neuron-specific beta-III Tubulin Antibody (1:50, Cat no. MAB1195; R&D Systems, Minneapolis, MN, USA) overnight at 4°C and then with donkey anti-mouse IgG (H+L) highly cross-adsorbed secondary antibody, Alexa Fluor 488 (1:500, Cat no. A32766TR; Invitrogen, Carlsbad, CA, USA) for one hour. Confocal corneal nerve images were detected by Zeiss (LSM880; Zeiss, Oberkochen, Germany) with an objective lens ×40 magnification. Image J was used to calculate fluorescence intensity and steps are listed as follows: 1. Convert to 8-Bit; 2. Use the threshold tool to select the areas of interest; 3. Go to "Analyze" > Set Measurements to select "Area," "Integrated density," and "Limit to threshold Analyze"; 4. Click measurements to obtain integrated density as results. To normalize, select the results of Sham group as control and calculate the mean value of Sham group. The normalized value for each data point = (Experimental Value)/(Control Mean). Use the normalized values for further statistical analysis and comparisons.

Immunofluorescence Staining for Corneal Section

Seven days after drug treatment, the eyeballs were excised and fixated in 4% paraformaldehyde overnight. On the next day and the third day, the eyeballs were placed in 20% and 30% sucrose for gradient dehydration, respectively.

After dehydration, optimal cutting temperature embedding was performed and made slices in 10 µm thickness. Before staining the frozen sections, they were dried at room temperature (30 minutes) and washed with PBS solution three times for five minutes each time. A chemical pen was used to create a circle around the tissue. Then the slices were blocked with 3% BSA containing 0.1% Triton X-100 for one hour, and incubated overnight at 4°C with the primary antibodies ZO-1 (1:100, Cat no. ab221547; Abcam). After being washed in PBS three times, the slices were incubated for one hour with the secondary antibody donkey anti-rabbit IgG (H+L) highly cross-adsorbed secondary antibody, Alexa Fluor 555 (1:500, Cat no. A-31572; Invitrogen). Images were acquired using a fluorescence microscope (Leica, Wetzlar, Germany) with an objective lens ×40 magnification. Fluorescence intensity was quantified with ImageJ software as described above.

Open Field Test

The open field test is a task for evaluating anxiety-like behavior in rodents. The test apparatus consists of a square arena with the floor marked into two sections by concentric squares, respectively. The area is divided into peripheral area and central area. Test sessions are ten minutes in duration and are conducted under bright white light. Mice naturally prefer to perform activities peripheral area due to the fear of potential risk and the drive to optimize security. Anxiety-like behavior include increasing the duration of time spent in- and the number of entries into- the center area of the open field.[47] Track plots (red traces) and heat maps showing the frequency of entries into- and the time spent in- the central area.

Statistic

Statistical analyses were performed using Origin software package version 2017. Statistical significance was calculated

Investigative Ophthalmology & Visual Science

using one-way ANOVA. Data are shown as the mean ± SD. A P value <0.05 was considered a statistically significant difference between the two groups.

Role of Funders

The sources of funding did not influence the design of the study, the collection of data, the analysis of data, the interpretation of results, or the writing of the manuscript.

Results

Effect of α7nAChR Agonists on Corneal Epithelial Defect Healing and Ocular Surface Inflammation in DED

LGE has been well established to induce dry eye disease and corneal nerve abnormality.[19] After unilateral excision of the extraorbital lacrimal gland, mice were randomly distributed into different groups, receiving a concentration gradient of PNU-282987. As dry eye disease is characterized with tear film instability, inflammation and corneal neurosensory abnormality in ocular surface.[48] After seven days' treatment, corneal fluorescein staining, phenol-red thread tear test, and corneal sensitivity tests were carried out (Fig. 1A). Results indicated that 1 mM PNU was the ideal concentration to alleviate DED symptoms, with minimal corneal epithelial injury, with a corneal fluorescein staining score of 0.67 ± 0.82 and restored corneal sensitivity (3.67 cm ± 1.25 cm) compared to those of all other groups (Fig. 1B). A significant reduction in tear production was observed in DED mice when compared to sham animals. Next, we set out to determine the effect of 1 mM PNU-282987 on DED mice. Mice were randomly distributed into different groups, receiving LGE + PBS, LGE + PNU-282987, LGE + MLA, LGE + PNU-282987 + MLA for seven days, named LGE, PNU, MLA, and PNU + MLA respectively. Dry eye disease is mainly characterized by ocular surface inflammation. Matrix metalloproteinase 9 is a proteinase secreted by the corneal epithelium that can compromise the barrier function of the corneal epithelium and contribute to the inflammatory process in DED.[49] Furthermore, quantitative real-time PCR (qRT–PCR) of corneal and conjunctival tissues demonstrated that PNU-282987 treatment resulted in a reduction of mRNA levels of *Mmp9* and three classic inflammatory cytokines, including *IL-1β, IL-6, TNF-α* compared to the LGE group ($P < 0.01$, $P > 0.05$, $P < 0.0001$, $P < 0.001$, respectively) (Figs. 1C–F). Specifically, in the LGE group, *Mmp9* expression increased by 2.67-fold compared to sham group ($P < 0.05$). Mice treated with PNU-282987 restored *Mmp9* levels to sham group ($P < 0.05$). In contrast, MLA administration resulted in a 1.36-fold increase in *Mmp9* expression relative to the LGE group, while the PNU-282987 + MLA group partially attenuated this effect, although this difference was not statistically significant (Fig. 1C). Similarly, PNU-282987 treatment reduced *IL-1β* expression to 48% of the levels observed in the LGE group (Fig. 1D). Conversely, MLA treatment led to a 1.18-fold increase in *IL-1β* expression compared to the LGE group, whereas the PNU-282987 + MLA group partially mitigated this effect ($P > 0.05$). Furthermore, *TNF-α* mRNA levels were significantly elevated in the LGE group but were normalized to sham group levels following PNU-282987 treatment (Fig. 1E). The PNU-282987 + MLA group exhibited a moderate reduction in *TNF-α* levels ($P < 0.05$), comparable to those in the control group. Lastly, *IL-6* expression was elevated by 4.2-fold in the LGE group compared to sham group. PNU-282987 treatment restored *IL-6* levels ($P < 0.05$), whereas the PNU-282987 + MLA group showed a partial but nonsignificant reduction in *IL-6* expression ($P > 0.05$) (Fig. 1F). To further investigate the effect of α7nAChR agonists on barrier function and nerve innervation.

We analyzed the level of superficial epithelial layers for the tight junction protein ZO-1 (Figs. 1G, 1H). ZO-1 staining indicated a reduced intensity in the LGE group compared to the sham group. Conversely, treatment with PNU-282987 resulted in an increased intensity, suggesting a significant improvement in barrier function following this treatment.

Next, we proceed to analyze the change of β-III tubulin (TUBB3), a neuronal marker involved in neurogenesis[50] was assessed. We observed a severe disruption of nerve ending in LGE group in contrast to SHAM (Figs. 1I, 1J). PNU-282987 treatment restored corneal nerve innervation relative to LGE group; however, this effect was diminished by the combination administration of PNU-282987 with MLA. Altogether, these results indicated that the administration of α7nAChR agonists reduced the ocular surface inflammation, restored corneal neurosensory function and promoted barrier reconstruction.

The Activation of α7nAChR Suppresses Inflammation Via Inhibiting M1-Macrophage Polarization

To identify potential downstream targets of α7nAChR agonists treatment, we analyzed alterations in corneal gene expression and signaling pathways using RNA-sequencing after seven days' treatment after LGE modeling. Different gene expression analysis revealed distinct disparities, with 108 genes up-regulated and 94 genes down-regulated in LGE versus SHAM group, and 97 genes displaying up-regulation and 58 genes down-regulation in LGE group versus PNU-282987 (Supplementary Fig. S2A). Additionally, the Venn diagram indicates the intersection of three groups (PNU-282987/LGE/sham), and 10 genes were overlapped among three groups (Supplementary Fig. S2B). Subsequently, gene ontology enrichment analysis of LGE group versus PNU-282987 group yielded enriched gene sets that were highly associated with immunoinflammation gene ontology terms (e.g., immune system process [$P = 8.06E-19$], innate immune response [$P = 4.63E-15$], type I interferon-mediated signaling pathway [$P = 4.86E-10$], and immune response [$P = 7.83E-07$]) (Fig. 2A). Similarly, in LGE versus SHAM group, GO terms was also enriched in immunoinflammation (Supplementary Fig. S2C). Furthermore, Wikipathways analysis of corneas of LGE group compared to PNU-282987 group was performed (Fig. 2B). Five enrichments pathways among top 20 arouse our interests, including macrophage markers, BDNF pathway, and matrix metalloproteinases. All these indicated a potential relationship between macrophage-related immune response and neuroenvironmental alteration in dry eye disease (Fig. 2B).

To further verify the effect of PNU-282987 on macrophage regulation, we firstly conducted in vitro flow cytometry experiments. After LPS stimulation, RAW264.7 cells (a mouse macrophage cell line) were treated with α7nAChR agonist and antagonist. The gating strategy were shown in Supplementary Figure S3. The results showed that on LPS stimulation, the expression of α7nAChR of macrophages in LPS group increased significantly compared to control group

Investigative Ophthalmology & Visual Science

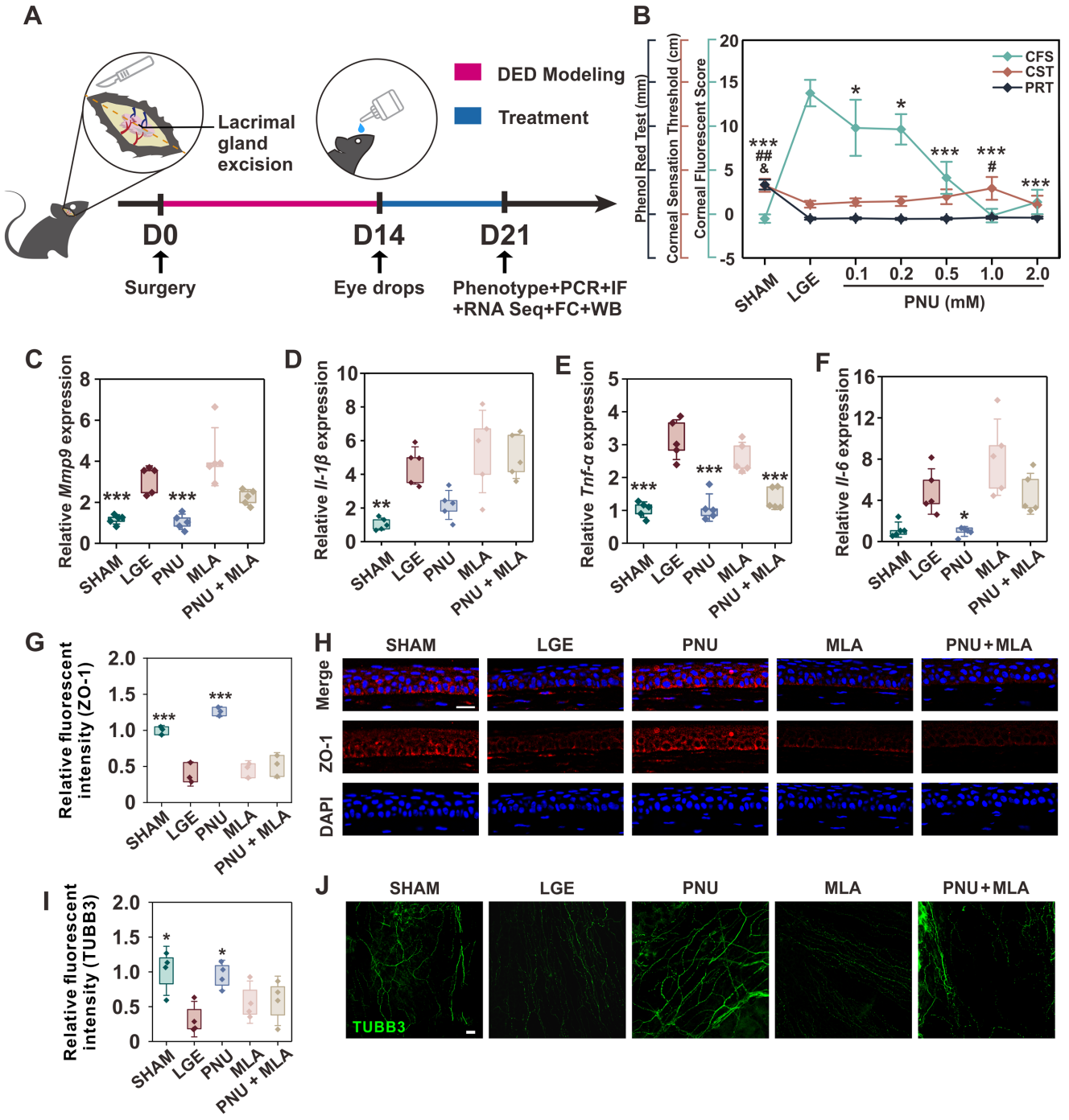

Figure 1. Effect of α7nAChR agonists on corneal epithelial defect healing and ocular surface inflammation in DED. (**A**) Schematic diagram of procedure on LGE-induced DED model. (**B**) The concentration gradient experiment of PNU-282987 (0.1, 0.2, 0.5, 1 and 2 mM). Mice were divided into seven groups, a sham group and LGE group treated with PBS (LGE) and different concentration of PNU-282987 (PNU). The best PNU-282987 concentration was determined by corneal fluorescein staining, corneal sensation threshold (CST) and phenol red thread tear test (PRT). (**C–K**) Mice were divided into five groups, sham group and LGE group treated with PBS (LGE), 1 mM of PNU-282987 (PNU), α7nAChR antagonist MLA, and PNU-282987 plus MLA (PNU + MLA). (**C–F**) Expression of inflammatory cytokine mRNA levels, including *MMP9, IL-1β*, *IL-6,* and *TNF-α* detected by RT-qPCR in cornea and conjunctiva; $n = 5$; n, number of eyeballs. (**G**, **H**) Representative confocal images of ZO-1 in the central corneal epithelium and relative fluorescent intensity. $n = 5$; n, number of eyeballs. *Scale bars*: 50 µm. (**I**, **J**) Representative confocal images of TUBB3+ nerves in the central cornea and relative fluorescent intensity. $n = 5$; n, number of eyeballs. *Scale bars*: 50 µm. CSF, corneal fluorescein staining. The statistical significance was determined using the analysis of One-way ANOVA analysis. Results are expressed as mean ± SD. n.s = not significant; *, groups compared to LGE, $^{*}P < 0.05$; $^{**}P < 0.01$; $^{***}P < 0.001$. See also Supplementary Figure S1.

Investigative Ophthalmology & Visual Science

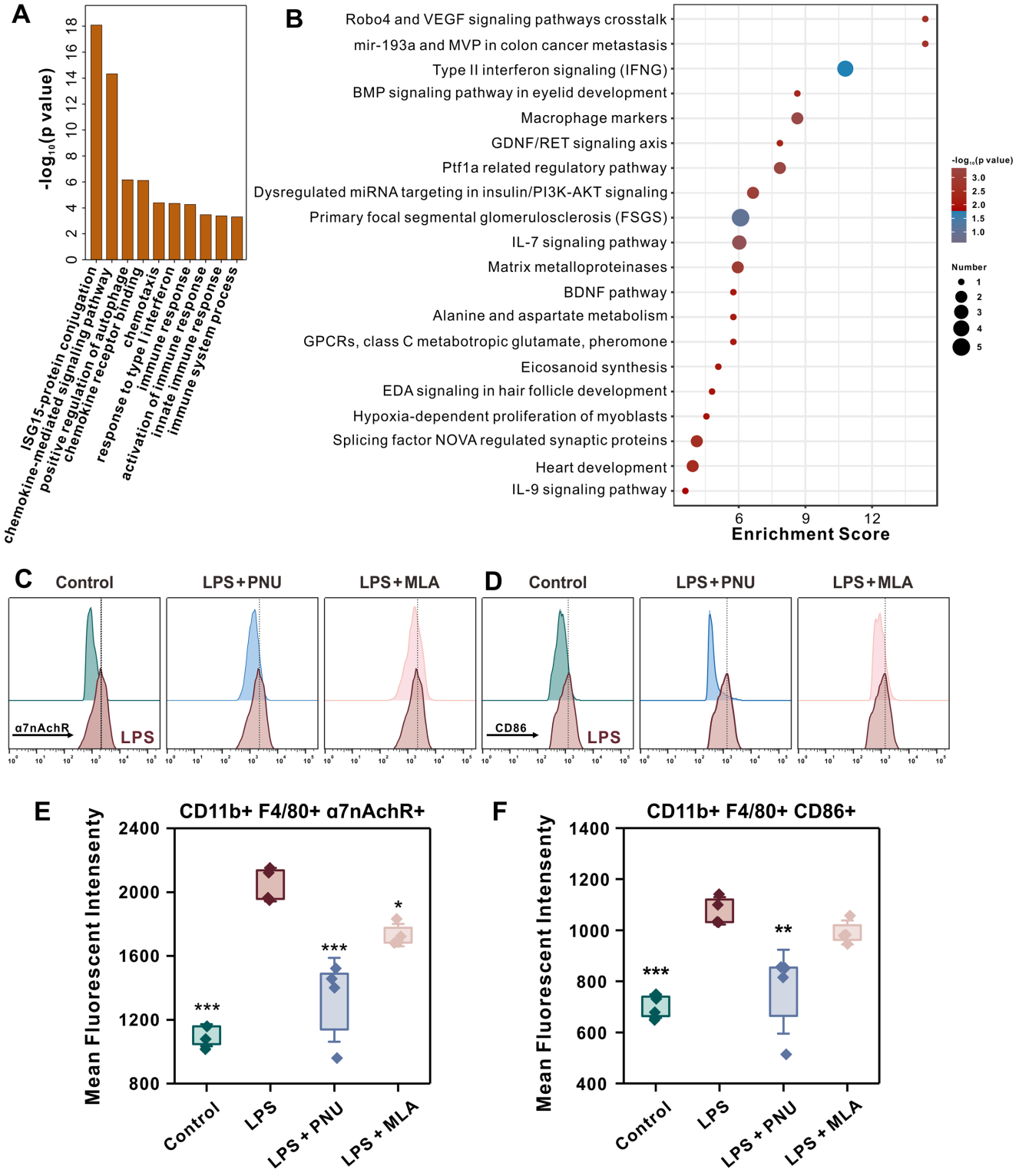

Figure 2. The α7nAChR agonists modulate macrophage-related immunoinflammatory response. Mice were divided into three groups, sham group and LGE group treated with PBS (LGE) and PNU-282987 (PNU) group. (**A**) Gene ontology (GO) analysis highlighting differential pathways in PNU-282987 treated cornea versus LGE cornea. (**B**) Bubble chart of Wikipathway analysis highlighting enrichments in macrophage-related immune response and neuroenvironmental alteration in PNU-282987 treated cornea versus LGE cornea. (**C–F**) RAW264.7 cells were divided into four groups: control (untreated), LPS, LPS + PNU-282987, LPS + MLA. Cells were harvest 12 hours after LPS stimulation. $n = 4$. (**C**, **D**) The representative histogram of α7nAChR (**C**) and CD86 (**D**) in RAW264.7 cells at 12 hours after LPS stimulation. (**E**, **F**) Quantitative analysis of corresponding mean fluorescent intensity of $\alpha7nAChR^+$ RAW264.7 cells (**E**) and $CD86^+$ RAW264.7 cells (**F**). The statistical significance was determined using the analysis of one-way ANOVA analysis. Results are expressed as mean ± SD. n.s = not significant; *, groups compared to LGE, $^*P < 0.05$; $^{**}P < 0.01$; $^{***}P < 0.001$. See also Supplementary Figure S2.

Investigative Ophthalmology & Visual Science

($P < 0.001$), whereas the use of PNU-282987 returned to the level equivalent to control group (Fig. 2C, 2E). The activation of α7nAChR receptor has been reported to suppress the M1 macrophage polarization.[22] CD86 are membrane surface molecule maker of M1. We assessed the level of $CD86^+$ RAW264.7 cells and found that the activation of α7nAChR remarkably down-regulated the mean fluorescence intensity (MFI) of $CD86^+$ RAW264.7 cells when compared to that in LPS-treated group, which was reversed by MLA (Figs. 2D, 2F).

To further investigate the activation effect of α7nAChR on macrophage in DED in vivo, we used clodronate liposomes, a specialized drug-delivery system designed to deplete macrophages, to evaluate the interaction between α7nAChR agonists and macrophages. Fourteen days after surgery, mice were randomly divided into SHAM + PBS, LGE + PBS, LGE + PNU-282987, LGE + MLA, LGE + PNU-282987 + MLA, LGE + Clodronate, LGE + Clodronate + MLA for seven days, named sham, LGE, PNU, MLA, PNU + MLA, clodronate, and clodronate + MLA, respectively. After seven days treatment, the cornea and conjunctiva of the mice were harvested to perform flow cytometry. Data revealed that an increase MFI of α7nAChR on macrophages was seen in LGE group compared to sham group (248.8 ± 70.6 vs. 107.1 ± 24.3, $P = 0.004$), whereas the PNU-282987 returned the level of the α7nAChR to normal level compared with LGE group (116.2 ± 18.8, $P = 0.007$). The MFI in MLA group was still in a relatively high level than the LGE group (201.8 ± 19.3 vs. 248.8 ± 70.6, $P > 0.05$). In the clodronate group, there was a decrease in MFI of α7nAChR in comparison to the LGE group (132.0 ± 22.8, $P = 0.03$) whereas the combination of clodronate and MLA increased the level (178.5 ± 75.6) (Figs. 3A, 3C). We further determined the MFI of CD86 protein on $CD11b^+$ $F4/80^+$ macrophages. In LGE group, the MFI of CD86 significantly increased in response to lacrimal gland excision, compared to the sham group (2920.8 ± 307.9 vs. 1509.5 ± 135.6, $P < 0.001$). Excitingly, the administration of PNU-282987 inhibited the MFI of CD86 (1500.3 ± 77.8, $P < 0.001$) on macrophage compared to LGE group, whereas the MLA group presented a high MFI comparable to LGE group (3242.0 ± 679.0, $P > 0.05$). Mice treated with clodronate showed a decrease in the MFI of CD86 compared to LGE group (1853.2 ± 170.6, $P < 0.01$); however, the combination used of clodronate and MLA still presented a lower intensity of CD86 than LGE group (1938.3 ± 368.5, $P < 0.01$) (Figs. 3B, 3D). This could be explained if the majority of macrophage had been depleted after administration of clodronate; therefore the use of MLA failed to reverse the trend. These results confirmed that the activation of α7nAChR accelerated the resolution of inflammation and nerve abnormality in ocular surface via down-regulating M1-type proinflammatory macrophage.

The α7nAChR Agonists Modulate Macrophage-Related Immunoinflammation Response

Inspired by the finding of flow cytometry results, we investigate whether α7nAChR agonists could modulate the macrophage-related immunoinflammation response. The expression mRNA level of macrophage- and neurofunction-related genes after activation of α7nAChR in DED was assessed. ADGRE1/F4/80 (adhesion G protein-coupled receptor E1) was the surface marker of macrophage. The CC chemokine receptor (CCR)-7 expression by corneal macrophage is known for its central role in facilitating adaptive immunity.[51] Neuropeptide Y (NPY) is a peptide thought to be critical in anti-nociceptive signaling during inflammatory and neuropathic pain.[52] Figures 3E through 3G showed changes in levels of *Adgre1, Ccr7,* and *Npy* mRNA levels in all groups. Results displayed that activation of α7nAChR receptor, the PNU-282987 group markedly down-regulated the mRNA expression of *Adgre1, Ccr7* compared to the LGE group ($P < 0.01$ and $P < 0.001$, respectively), and up-regulated the mRNA expression of *NPY* ($P < 0.05$). Next, we quantified the protein level of CD11b, a macrophage marker. Western blot results showed that the expression of CD11b was greatly increased in the LGE group, a 2.32-fold increase compared to the sham group, suggesting the obvious increased macrophage. However, the expression of CD11b in the PNU-282987 group was two times lower than that in LGE (Fig. 3H, 3I). Clodronate group showed a decrease of CD11b expression compared to LGE (0.82-fold vs. 2.32-fold, $P < 0.01$), whereas the combination of MLA counteracted the clodronate effect. Transient receptor potential vanilloid-1 (TRPV1) is a representative pain receptor activated by multiple stimuli. The suppression of TRPV1 has been reported to ameliorate dry eye–induced neuropathic ocular pain.[53] Here, a 2.69-fold high expression of TRPV1 in LGE group compared to SHAM ($P < 0.05$); whereas a down-regulation of TRPV1 expression was noted in the PNU-282987-treated group ($P < 0.05$). The clodronate group showed a decrease trend of TRPV1 expression (1.64-fold), and the combination of clodronate with MLA slightly increased the expression (2.11-fold) (Figs. 3I, 3J). These results confirmed that the activation of α7nAChR accelerated the resolution of inflammation and nerve abnormality in ocular surface via down-regulating M1-type proinflammatory macrophage. These results confirm that the activation of α7nAChR decrease ocular surface inflammation via modulating macrophage-related immunoregulation.

α7nAChR Agonists Restore Sensory Innervation and Alleviate Anxiety-Like Behaviors

To determine whether the activation of α7nAChR could affect the phenotype of corneal integrity and neuronal sensory abnormalities in dry eye disease, we first proceeded to observe the change of cornea epithelium after seven days treatments via corneal fluorescein staining. Results showed that LGE group remained strong fluorescence with a staining score of 13.17 ± 3.25 (Figs. 4A, 4E). In comparison, both PNU-282987 and clodronate restored the corneal epithelium integrity with a significant lower corneal fluorescence staining score of 0.67 ± 0.82 and 1.00 ± 0.89, respectively ($P < 0.001$); yet the MLA group, the PNU-282987 + MLA group, and the clodronate + MLA group still displayed intense punctate epithelium injury with a staining score of 11.67 ± 2.58, 13.33 ± 2.73, and 10.17 ± 2.04, respectively (Fig. 4E). Next, we measured corneal sensitivity using an esthesiometer. As shown in Figure 4F, the sensory function was preserved in PNU-282987 treated group compared to LGE group (3.67 cm ± 1.25 cm vs. 1.33 cm ± 0.41 cm, $P < 0.001$). Clodronate also restored corneal sensation to 2.92 cm ± 1.02 cm threshold. In contrast, the sensory function was worse in the MLA group, PNU-282987 + MLA group, and clodronate + MLA group. In addition, immunofluorescent analysis showed that $TUBB3^+$ nerve density was dramat-

Investigative Ophthalmology & Visual Science

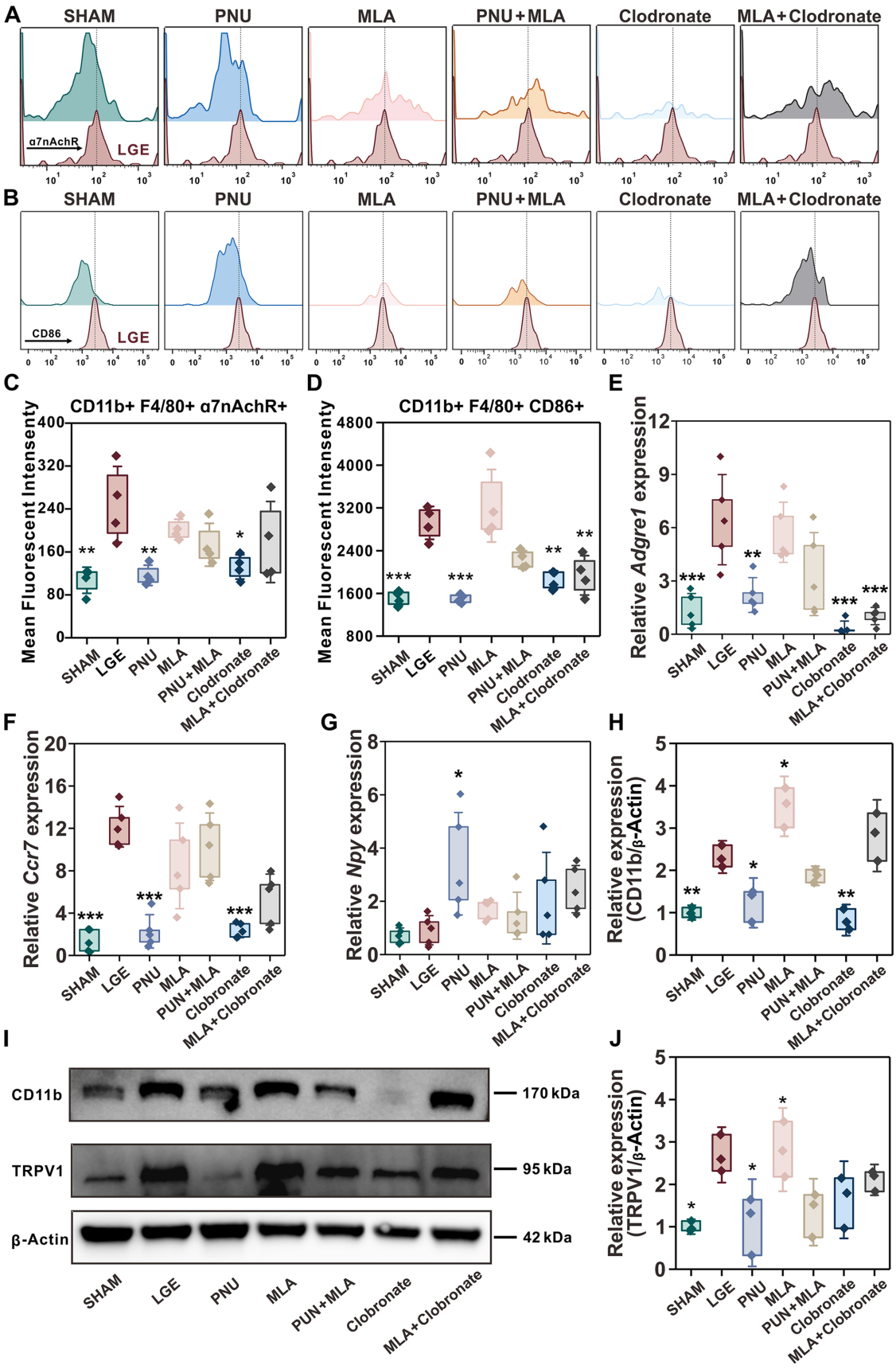

Figure 3. The activation of α7nAChR suppresses inflammation via inhibiting M1-macrophage polarization. Mice were divided into seven group: SHAM, LGE, LGE + PNU-282987, LGE + MLA, LGE + PNU- 282987 + MLA, LGE + Clodronate, LGE + Clodronate + MLA. (**A**, **B**) The representative histogram of α7nAChR (**A**) and CD86 (**B**) in $CD11b^+$ $F4/80^+$ macrophages in the cornea and conjunctiva. (**C**, **D**) Quantitative analysis of corresponding mean fluorescent intensity of $\alpha7nAChR^+$ macrophages cells (**C**) and $CD86^+$ macrophages

Investigative Ophthalmology & Visual Science

(**D**). (**E–G**) Expression of macrophage-related protein and neuropeptide mRNA levels, including *Adgre1, Ccr7,* and *Npy* detected by RT-qPCR in cornea and conjunctiva. $n = 5$; n, number of eyeballs. (**H**) Western blotting of CD11b and TPRV1 in cornea and conjunctiva. β-Actin was used as a housekeeping standard. (**I**, **J**) Densitometry analysis of western blots. The bands of CD11b (H) and TPRV1 (J) were analyzed with Image software. $n = 3$; n, number of eyeballs. The statistical significance was determined using the analysis of one-way ANOVA analysis. Results are expressed as mean ± SD. n.s = not significant; *, groups compared to LGE, $^{*}P < 0.05$; $^{**}P < 0.01$; $^{***}P < 0.001$. See also Supplementary Figure S3.

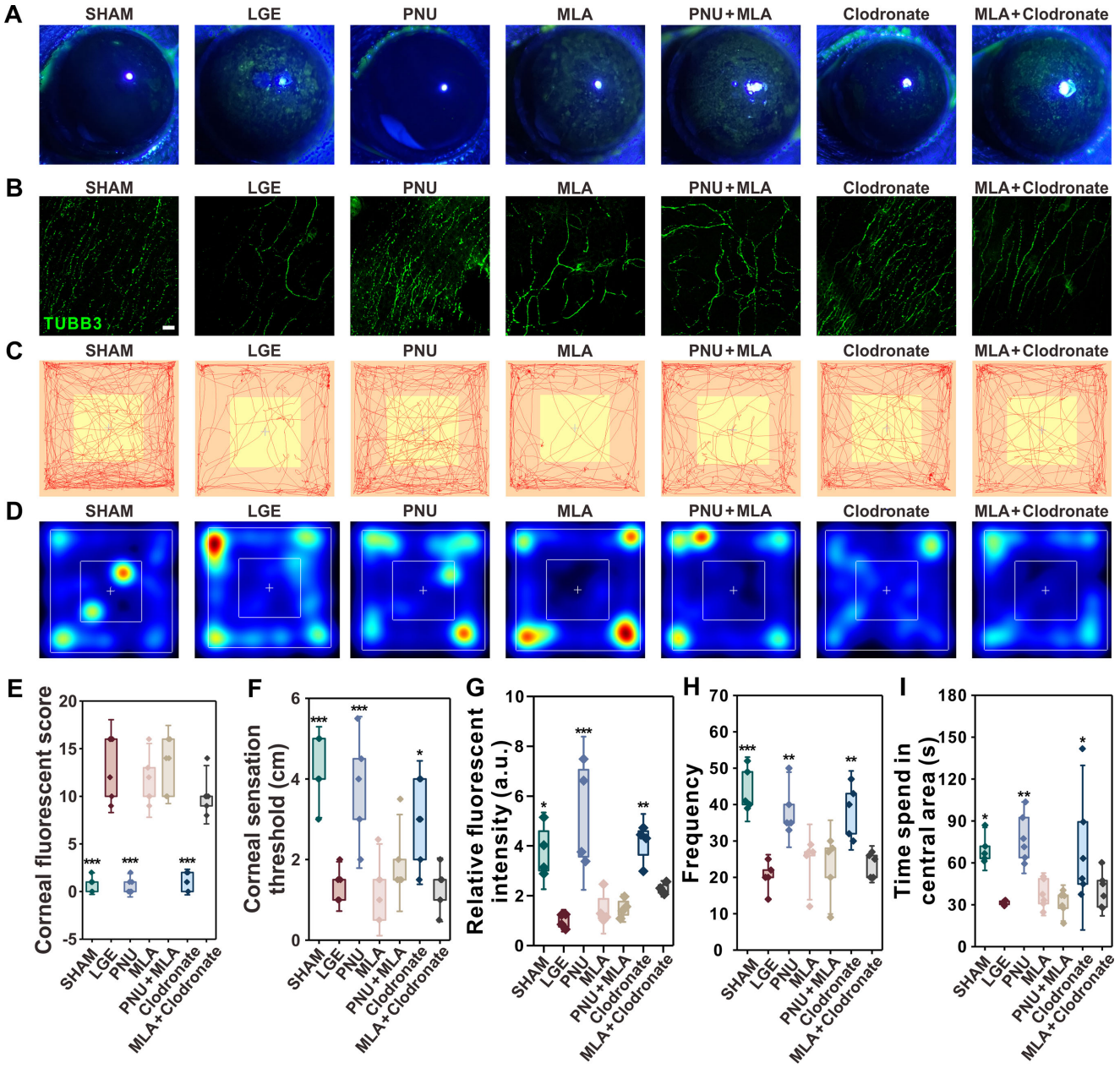

Figure 4. The activation of α7nAChR restores sensory innervation and reduce anxiety-like behaviors. (**A**) Representative fluorescein sodium staining images (**B**) Representative confocal images of TUBB3^{+} nerves in the central corneal epithelium in each group. *Scale bars*: 25 µm. (**C**, **D**) Open-field tests were used to observe the behavioral patterns and a 10 minutes test for each mice were performed. $n = 5$; n, number of mice. (**C**) Representative track plots of open-field test. The *central yellow square* was denominated "central zone" and the *orange periphery*, "border zone." (**D**) Representative heat maps showing time spent in each area of the open field chamber. (**E**) Relative fluorescent intensity of TUBB3^{+}. $n = 3$; n, number of eyeballs. (**F**) Quantitative analysis of the corneal sensation threshold. (**G**) Relative fluorescent intensity of TUBB3^{+}. (**H**) The frequency travelled from the peripheral area to the central area. (**I**) Time spend in central area. The statistical significance was determined using the analysis of one-way ANOVA analysis. Results are expressed as mean ± SD. n.s = not significant; *, groups compared to LGE, $^{*}P < 0.05$; $^{**}P < 0.01$; $^{***}P < 0.001$.

Investigative Ophthalmology & Visual Science

ically reduced in the LGE group in contrast to the sham group (Figs. 4B, 4G). Surprisingly, corneas in PNU-282987 group and clodronate group were extensive innervated by TUBB3$^+$ compared to LGE group ($P < 0.001$ and $P < 0.01$), whereas clodronate plus MLA inhibited nerve restoration. Next, we questioned whether the stimulation of α7nAChR agonist modulate the behavioral patterns of mice. Because clinical data suggest that DED is often associated with anxiety and depression syndromes,[54] the open field test was performed. A comparison of rearing frequency (Figs. 4C, 4H) showed that a decrease frequency was observed in LGE group when compared to the sham group (20.2 ± 4.0 vs. 44.2 ± 5.9, $P < 0.001$). Surprisingly, the administration of PNU-282987 and clodronate increased the frequency of rearing compared to LGE (38.6 ± 6.9 vs. 20.2 ± 4.0, $P < 0.01$; 38.4 ± 7.2 vs 20.2 ± 4.0, $P < 0.01$), whereas there was no significant difference between MLA and LGE. Similarly, evaluation of time spent in central area revealed that a noticeable increase of time in mice treated with PNU-282987 and clodronate when compared to LGE (78.0 ± 17.1 seconds vs. 31.2 ± 1.4 seconds, $P < 0.001$; 70.9 ± 39.3 seconds vs. 31.2 ± 1.4 seconds, $P < 0.05$) (Figs. 4D, 4I).

Discussion

DED is a multifactorial disease characterized with tear film instability, ocular inflammation and corneal nerve abnormalities.[1] In the present study, we demonstrated that α7nAChR agonists down-regulate ocular inflammatory response by inhibiting macrophage polarization toward M1-type in murine DED model. Furthermore, the administration of α7nAChR agonists modulates corneal nerve abnormality and alleviates anxiety-like behavior associated with persistent DED.

The resolution of inflammation exerted by the activation of α7nAChR contributed to the repair of corneal epithelial defects. The α7nAChR, found on immune cells, has emerged as a promising therapeutic target for inflammatory diseases. Manipulation of autonomic nervous system inputs to the wounded cornea have represented an alternative approach to the treatment of wound healing. Specifically, acetylcholine released from pulmonary vagal nerve endings can activate macrophages expressing the α7nAChR, leading to the suppression of NF-kB activity and a reduction in pro-inflammatory cytokine production, which finally lessened the extent of lung inflammation and injury.[55] Of note, the recruitment of α7nAChR$^+$ CD11b$^+$ cells has been shown to attenuate LPS and *Escherichia coli*–induced acute lung inflammatory injury.[56] A study that used a corneal abrasion model also showed that topical administration of α7nAChR agonist promoted re-epithelialization and inhibited macrophage influx and release of inflammatory cytokines.[23] In present study, the activation of α7nAChR was essential for resolving corneal defects and enhancing barrier function, as indicated by ZO-1 expression. Additionally, ACh axis in corneal epithelium plays an important role in regulation and coordination of distinct activities of corneal epithelial cells in re-epithelialization. In the mouse cornea, the main expression of M(2,5)AChRs and α(1,4,7)nAchRs has been identified.[23] Ex vivo experiments demonstrated that activating α7nAChR initiates the Ras-Raf-MEK-ERK cascade, thereby accelerating corneal re-epithelialization through increased E-cadherin expression.[57] Future study exploring the effects of α7nAChR activation on corneal epithelium in vivo would clarify the role of α7nAChR agonists in wound healing more comprehensively.

Importantly, the autoimmune response of DED is characterized by the initial ingress of macrophages into the cornea and subsequent homing of macrophages to the draining lymph nodes.[58] Macrophages are key immune cells recruited to the cornea during ocular surface disease. Broadly, macrophages are classified into two main categories: pro-inflammatory M1-like or anti-inflammatory M2-like phenotype.[59] In DED, M1 macrophage polarization is typically driven by pro-inflammatory cytokines such as IFN-γ and TNF-α, which are often elevated in the tear film and ocular surface of DED patients.[60] M1 macrophages contribute to tissue damage by releasing pro-inflammatory mediators, exacerbating ocular surface inflammation and epithelial cell apoptosis. Conversely, M2 macrophage polarization is induced by anti-inflammatory cytokines such as IL-4, IL-13, and IL-10, which present during the resolution phase of inflammation or in response to tissue repair signals.[61] The α7nAChR activation has been implicated in the modulation of immune cell function, especially the macrophages. The expression of α7 subunit in macrophages is essential for inflammation suppression.[22] The up-regulated expression of α7nAChR was observed in alveolar type II cells and α7nAChR$^+$ macrophages in response to LPS-induced acute lung injury.[56,62] Previous study found that the topical administration of β-2 adrenergic receptor agonist enhanced the expression of the proinflammatory genes in the CD64$^+$CCR2+ macrophages sorted from injured corneas. In contrast, the topical administration of an α7nAChR agonist further enhanced the expression of the anti-inflammatory genes in the CD64$^+$CCR2$^-$ macrophages.[23] Notably, in our study, activation of the α7nAChR, as seen in the PNU-282987-treated group, suppressed M1 macrophage polarization and release of related immunoinflammation factor. Interestingly, in present study, we observed an increase in endogenous α7nAChR expression in RAW264.7 cell in response to LPS stimulation compared to the control group in vitro. Similarly, in an LGE-induced DED model in vivo, we also noted increased α7nAChR expression. This phenomenon, an increased expression of α7nAChR, could be considered as a protective response to external harmful stimuli,[56,62] as macrophages expressing α7nAChR demonstrate anti-inflammatory effects upon activation.[22] Notably, this increase was counteracted in the PNU-282987-treated group and clodronate group, which may account for their observed anti-inflammatory effects.

Recently, corneal nerve abnormalities, including morphological and functional changes, have been highlighted in the development of DED.[6,63] Attempts for testing novel therapies with neuroregenerative potential have been made,[50] including insulin growth factor-1,[64] pigment epithelium–derived factor,[65] and so on; however, results are limited. The activation of α7nAChRs reversed the loss of cornea nerve, which was also detected in LGE mice treated with clodronate. Importantly, α7nAChR, a key neurotransmitter, interacts the nervous and immune systems to exert the anti-inflammatory function. Because endings of cornea nerve rely entirely on corneal epithelial cells for support[66] and their impairment coincides with corneal epitheliopathy development, it is possible that the activation of α7nAChR creates a nerve-friendly environment via suppressing the proinflammatory cytokines production, M1 macrophage infiltration and promoting corneal innervation and epithelium integrity. Moreover, there is a decrease in mechanical sensitivity. The

Investigative Ophthalmology & Visual Science

finding of increase TRPV1 expression may help explain this phenomenon, because previous reports on TRPV1 activity have also been linked to corneal nerve degeneration in dry eye.[17] In addition, increased TRPV1 protein levels enhanced nocifensive behavior has been reported for DED rats.[67] The down-regulation of TRPV1 is response for alleviation of anxiety-like behaviors.[28] A similar trend was also observed in mice treated with clodronate. These results corroborated showed that α7nAChR agonists restore sensory innervation and alleviate anxiety-like behaviors via mediating the immune microenvironment in the context of DED.

Currently, there is a lack of direct human studies on the specific role of α7nAChR in DED. Varenicline solution nasal spray 0.03 mg, a nicotinic acetylcholine receptor agonist approved by the Food and Drug Administration for dry eye disease, has demonstrated efficacy in modulating T-cell–mediated inflammation. A recent pilot study showed that varenicline solution nasal spray significantly reduces tear levels of Th1-associated cytokines (IL-2, IFN-γ, and TNF-α) and Th17-associated IL-17A in Sjögren's syndrome patients, supporting its potential in Th1/Th17-driven DED.[68] This supports the potential of α7nAChR targeting in Th1/Th17-driven DED and provides indirect evidence for the clinical relevance of our research. Given the established role of α7nAChR in modulating macrophage polarization and inflammation,[69] we hypothesize that α7nAChR agonists would exhibit similar therapeutic effects in benzalkonium chloride (BAC) and desiccating stress (DS) models, where T cells are thought to drive the inflammatory response. The α7nAChR agonist may act through both indirect regulation via macrophage-dependent T-cell modulation and direct effects on T cell–expressed α7nAChRs, influencing both effector T cell and Treg development. Various animal models of DED, including BAC-induced,[70] DS-induced,[71] and LGE-induced model has been characterized with Th1 and Th17 cell response. Given the established role of α7nAChR in modulating macrophage polarization and inflammation, we hypothesize that α7nAChR agonists would exhibit similar therapeutic effects in BAC and DS models, where T cells are thought to drive the inflammatory response. The α7nAChR agonist may act through both indirect regulation via macrophage-dependent T-cell modulation and direct effects on T-cell–expressed α7nAChRs, influencing both effector T-cell and Treg development.[72]

Together, these observations demonstrate that α7nAChR signaling plays a significant neuroimmune role in DED and the activation of α7nAChR restored corneal epithelial integrity and attenuated addressing nerve abnormalities through a mechanism that involves modulating anti-inflammatory macrophages and reducing pro-inflammatory macrophages. The findings encourage further exploration of α7nAChR in resolution of inflammation and restoration of neuronal regulation abnormalities.

Acknowledgments

Supported by National youth talent support program (QWF158001), National Natural Science Foundation of China (82271044), the Shanghai Oriental Talent Program (2024), the Fudan University Young Clinical Researcher Training Program (2023) of X.Z., National Science Fund for Distinguished Young Scholars (82425015), National Natural Science Foundation of China (82171102), National Key Research and Development Program of China (2023YFA0915000), (the "Dawn" Program of) Shanghai Municipal Education Commission (24SG11), Shanghai Science and Technology Innovation Action Plan for Cell and Gene Therapy (24J22800500), Shanghai Science and Technology Innovation Action Plan for Advanced Materials (24CL2900802), Shanghai Municipal Commission of Health (20254Z0019), Shanghai Medicine and Health Development Foundation and Shanghai Medical Innovation Research Program (22Y21900900) of J.H., National Key R&D Program of China (2023YFB3208200), the National Natural Science Foundation of China (22393932, T2321005, 21825402), the Science and Technology Development Fund, Macau SAR (0002/2022/AKP, 0115/2023/RIA2) and the Program for Jiangsu Specially Appointed Professors to Professor Yao He, a project funded by the Priority Academic Program Development of Jiangsu Higher Education Institutions (PAPD), 111 Project and Collaborative Innovation Centre of Suzhou Nano Science and Technology (NANO-CIC) of Y.H., National Natural Science Foundation of China (22204117, 22474084) of B.C., Natural Science Foundation of Gansu Province Science and Technology Program (23JRRA1460) of K.Y.

Author Contributors: Conceptualization, X.Z., J.H. and Y.H.; Methodology, K.Y., X.Z., J.H. and Y.H.; Investigation, X.Z., J.H. and Y.H.; Writing Original Draft, Y.W., Y.Z.; Writing X.Z., Y.W., Y.Z. and B.C.; Review & Editing, X.Z., J.H. and Y.H.; Funding Acquisition, X.Z. and J.H.; Resources, X.Z., J.H. and Y.H.; Supervision, X.Z., J.H. and Y.H.

Data Sharing Statement: RNA sequencing data during the current study are available in GEO repository, https://www.ncbi.nih.gov/geo/query/acc.cgi?acc=GSE263136.

Disclosure: **X. Zhou**, None; **Y. Wu**, None; **Y. Zhang**, None; **B. Chu**, None; **K. Yang**, None; **J. Hong**, None; **Y. He**, None

References

1. Craig JP, Nichols KK, Akpek EK, et al. TFOS DEWS II definition and classification report. *Ocul Surf*. 2017;15:276–283.
2. Stapleton F, Alves M, Bunya VY, et al. TFOS DEWS II epidemiology report. *Ocul Surf*. 2017;15:334–365.
3. Walter K. What is dry eye disease? *JAMA*. 2022;328:84.
4. Lu C, Fu J, Liu X, et al. Impacts of air pollution and meteorological conditions on dry eye disease among residents in a northeastern Chinese metropolis: a six-year crossover study in a cold region. *Light Sci Appl*. 2023;12:186.
5. Lu C, Fu J, Liu X, et al. Air pollution and meteorological conditions significantly contribute to the worsening of allergic conjunctivitis: a regional 20-city, 5-year study in Northeast China. *Light Sci Appl*. 2021;10:190.
6. Belmonte C, Nichols JJ, Cox SM, et al. TFOS DEWS II pain and sensation report. *Ocul Surf*. 2017;15:404–437.
7. Dermer H, Hwang J, Mittal R, Cohen AK, Galor A. Corneal sub-basal nerve plexus microneuromas in individuals with and without dry eye. *Br J Ophthalmol*. 2022;106:616–622.
8. Downie LE, Bandlitz S, Bergmanson JPG, et al. CLEAR—anatomy and physiology of the anterior eye. *Cont Lens Anterior Eye*. 2021;44:132–156.
9. Vereertbrugghen A, Galletti JG. Corneal nerves and their role in dry eye pathophysiology. *Exp Eye Res*. 2022;222:109191.
10. Guerrero-Moreno A, Liang H, Moreau N, et al. Corneal nerve abnormalities in painful dry eye disease patients. *Biomedicines*. 2021;9:1424.
11. Uchino Y, Uchino M, Mizuno M, Shigeno Y, Furihata K, Shimazaki J. Morphological alterations in corneal nerves of patients with dry eye and associated biomarkers. *Exp Eye Res*. 2023;230:109438.
12. Patel S, Hwang J, Mehra D, Galor A. Corneal nerve abnormalities in ocular and systemic diseases. *Exp Eye Res*. 2021;202:108284.

13. Leonard BC, Stewart KA, Shaw GC, et al. Comprehensive clinical, diagnostic, and advanced imaging characterization of the ocular surface in spontaneous aqueous deficient dry eye disease in dogs. *Cornea*. 2019;38:1568–1575.
14. Labbé A, Liang Q, Wang Z, et al. Corneal nerve structure and function in patients with non-Sjogren dry eye: clinical correlations. *Invest Ophthalmol Vis Sci*. 2013;54:5144–5150.
15. Vehof J, Sillevis Smitt-Kamminga N, Nibourg SA, Hammond CJ. Predictors of discordance between symptoms and signs in dry eye disease. *Ophthalmology*. 2017;124:280–286.
16. Guzmán M, Miglio M, Keitelman I, et al. Transient tear hyperosmolarity disrupts the neuroimmune homeostasis of the ocular surface and facilitates dry eye onset. *Immunology*. 2020;161:148–161.
17. Pizzano M, Vereertbrugghen A, Cernutto A, et al. Transient receptor potential vanilloid-1 channels facilitate axonal degeneration of corneal sensory nerves in dry eye. *Am J Pathol*. 2024;194:810–827.
18. Benitez-Del-Castillo JM, Moreno-Montañés J, Jiménez-Alfaro I, et al. Safety and efficacy clinical trials for SYL1001, a novel short interfering RNA for the treatment of dry eye disease. *Invest Ophthalmol Vis Sci*. 2016;57:6447–6454.
19. Fakih D, Zhao Z, Nicolle P, et al. Chronic dry eye induced corneal hypersensitivity, neuroinflammatory responses, and synaptic plasticity in the mouse trigeminal brainstem. *J Neuroinflammation*. 2019;16:268.
20. Lasagni Vitar RM, Bonelli F, Rama P, Ferrari G. Immunity and pain in the eye: focus on the ocular surface. *Clin Exp Immunol*. 2022;207:149–163.
21. Xu M, Li C, Zhao GQ, et al. The anti-inflammatory regulation of calcitonin gene-related peptide in mouse Aspergillus fumigatus keratitis. *Int J Ophthalmol*. 2020;13:701–707.
22. Wang H, Yu M, Ochani M, et al. Nicotinic acetylcholine receptor alpha7 subunit is an essential regulator of inflammation. *Nature*. 2003;421:384–388.
23. Xue Y, He J, Xiao C, et al. The mouse autonomic nervous system modulates inflammation and epithelial renewal after corneal abrasion through the activation of distinct local macrophages. *Mucosal Immunol*. 2018;11:1496–1511.
24. Frampton JE. Varenicline solution nasal spray: a review in dry eye disease. *Drugs*. 2022;82:1481–1488.
25. Wirta D, Vollmer P, Paauw J, et al. Efficacy and safety of OC-01 (Varenicline Solution) nasal spray on signs and symptoms of dry eye disease: the ONSET-2 Phase 3 Randomized Trial. *Ophthalmology*. 2022;129:379–387.
26. Esaki H, Deyama S, Izumi S, et al. Varenicline enhances recognition memory via α7 nicotinic acetylcholine receptors in the medial prefrontal cortex in male mice. *Neuropharmacology*. 2023;239:109672.
27. Alam J, de Paiva CS, Pflugfelder SC. desiccation induced conjunctival monocyte recruitment and activation—implications for keratoconjunctivitis. *Front Immunol*. 2021;12:701415.
28. Fakih D, Guerrero-Moreno A, Baudouin C, Réaux-Le Goazigo A, Parsadaniantz SM. Capsazepine decreases corneal pain syndrome in severe dry eye disease. *J Neuroinflammation*. 2021;18:111.
29. Mecum NE, Demers D, Sullivan CE, Denis TE, Kalliel JR, Meng ID. Lacrimal gland excision in male and female mice causes ocular pain and anxiety-like behaviors. *Sci Rep*. 2020;10:17225.
30. Shinomiya K, Ueta M, Kinoshita S. A new dry eye mouse model produced by exorbital and intraorbital lacrimal gland excision. *Sci Rep*. 2018;8:1483.
31. Zhou X, Zong Y, Zhang R, et al. Differential modulation of GABA(A) and NMDA receptors by an α7-nicotinic acetylcholine receptor agonist in chronic glaucoma. *Front Mol Neurosci*. 2017;10:422.
32. Webster MK, Cooley-Themm CA, Barnett JD, et al. Evidence of BrdU-positive retinal neurons after application of an Alpha7 nicotinic acetylcholine receptor agonist. *Neuroscience*. 2017;346:437–446.
33. Yang L, Dong C, Tian L, Ji X, Yang L, Li L. Gadolinium chloride restores the function of the gap junctional intercellular communication between hepatocytes in a liver injury. *Int J Mol Sci*. 2019;20.
34. Wu H, Xu X, Li J, Gong J, Li M. TIM–4 blockade of KCs combined with exogenous TGF–β injection helps to reverse acute rejection and prolong the survival rate of mice receiving liver allografts. *Int J Mol Med*. 2018;42:346–358.
35. Opperman KS, Vandyke K, Clark KC, et al. Clodronate-liposome mediated macrophage depletion abrogates multiple myeloma tumor establishment in vivo. *Neoplasia*. 2019;21:777–787.
36. Cortina MS, He J, Russ T, Bazan NG, Bazan HE. Neuroprotectin D1 restores corneal nerve integrity and function after damage from experimental surgery. *Invest Ophthalmol Vis Sci*. 2013;54:4109–4116.
37. Niu XH, Liu RH, Lv X, et al. Activating α7nAChR helps post-myocardial infarction healing by regulating macrophage polarization via the STAT3 signaling pathway. *Inflamm Res*. 2023;72:879–892.
38. Sugita J, Asada Y, Ishida W, et al. Contributions of Interleukin-33 and TSLP in a papain-soaked contact lens-induced mouse conjunctival inflammation model. *Immun Inflamm Dis*. 2017;5:515–525.
39. Li L, Li Y, Zhu X, et al. Conjunctiva resident $\gamma\delta$ T cells expressed high level of IL-17A and promoted the severity of dry eye. *Invest Ophthalmol Vis Sci*. 2022;63:13.
40. Chen S, Zhou Y, Chen Y, Gu J. Fastp: an ultra-fast all-in-one FASTQ preprocessor. *Bioinformatics*. 2018;34:i884–i890.
41. Kim D, Langmead B, Salzberg SL. HISAT: a fast spliced aligner with low memory requirements. *Nat Methods*. 2015;12:357–360.
42. Roberts A, Trapnell C, Donaghey J, Rinn JL, Pachter L. Improving RNA-Seq expression estimates by correcting for fragment bias. *Genome Biol*. 2011;12:R22.
43. Anders S, Pyl PT, Huber W. HTSeq—a Python framework to work with high-throughput sequencing data. *Bioinformatics*. 2015;31:166–169.
44. Love MI, Huber W, Anders S. Moderated estimation of fold change and dispersion for RNA-seq data with DESeq2. *Genome Biol*. 2014;15:550.
45. Yang Y, Chen M, Zhai Z, et al. Long non-coding RNAs Gabarapl2 and Chrnb2 positively regulate inflammatory signaling in a mouse model of dry eye. *Front Med (Lausanne)*. 2021;8:808940.
46. Kanehisa M, Araki M, Goto S, et al. KEGG for linking genomes to life and the environment. *Nucleic Acids Res*. 2008;36:D480–484.
47. Pentkowski NS, Rogge-Obando KK, Donaldson TN, Bouquin SJ, Clark BJ. Anxiety and Alzheimer's disease: behavioral analysis and neural basis in rodent models of Alzheimer's-related neuropathology. *Neurosci Biobehav Rev*. 2021;127:647–658.
48. Datta A, Lee JH, Flandrin O, et al. TRPA1 and TPRV1 Ion channels are required for contact lens-induced corneal parainflammation and can modulate levels of resident corneal immune cells. *Invest Ophthalmol Vis Sci*. 2023;64:21.
49. Lu Z, Liu T, Zhou X, et al. Rapid and quantitative detection of tear MMP-9 for dry eye patients using a novel silicon nanowire-based biosensor. *Biosens Bioelectron*. 2022;214:114498.
50. Efraim Y, Chen FYT, Cheong KN, Gaylord EA, McNamara NA, Knox SM. A synthetic tear protein resolves dry eye through promoting corneal nerve regeneration. *Cell Rep*. 2022;40:111307.

Investigative Ophthalmology & Visual Science

51. Kodati S, Chauhan SK, Chen Y, et al. CCR7 is critical for the induction and maintenance of Th17 immunity in dry eye disease. *Invest Ophthalmol Vis Sci*. 2014;55:5871–5877.
52. Khamar P, Nair AP, Shetty R, et al. dysregulated tear fluid nociception-associated factors, corneal dendritic cell density, and vitamin d levels in evaporative dry eye. *Invest Ophthalmol Vis Sci*. 2019;60:2532–2542.
53. Kikuchi K, Tagawa Y, Murata M, Ishida S. Effects of mirogabalin on hyperalgesia and chronic ocular pain in tear-deficient dry-eye rats. *Invest Ophthalmol Vis Sci*. 2023;64:27–27.
54. Kitazawa M, Sakamoto C, Yoshimura M, et al. The relationship of dry eye disease with depression and anxiety: a naturalistic observational study. *Transl Vis Sci Technol*. 2018;7:35.
55. Su X, Lee JW, Matthay ZA, et al. Activation of the alpha7 nAChR reduces acid-induced acute lung injury in mice and rats. *Am J Respir Cell Mol Biol*. 2007;37:186–192.
56. Zhao C, Yang X, Su EM, et al. Signals of vagal circuits engaging with AKT1 in α7 nAChR(+)CD11b(+) cells lessen E. coli and LPS-induced acute inflammatory injury. *Cell Discov*. 2017;3:17009.
57. Chernyavsky AI, Galitovskiy V, Grando SA. Molecular mechanisms of synergy of corneal muscarinic and nicotinic acetylcholine receptors in upregulation of E-cadherin expression. *Int Immunopharmacol*. 2015;29:15–20.
58. Bron AJ, de Paiva CS, Chauhan SK, et al. TFOS DEWS II pathophysiology report. *Ocul Surf*. 2017;15:438–510.
59. Xie M, Wu Y, Zhang Y, et al. Membrane fusion-mediated loading of therapeutic siRNA into exosome for tissue-specific application. *Adv Mater*. 2024;36:e2403935.
60. Wang HH, Chen WY, Huang YH, et al. Interleukin-20 is involved in dry eye disease and is a potential therapeutic target. *J Biomed Sci*. 2022;29:36.
61. Peng Y, Zhou M, Yang H, et al. Regulatory mechanism of M1/M2 macrophage polarization in the development of autoimmune diseases. *Mediators Inflamm*. 2023;2023:8821610.
62. Chen X, Zhang C, Wei T, et al. α7nAChR activation in AT2 cells promotes alveolar regeneration through WNT7B signaling in acute lung injury. *JCI Insight*. 2023;8(15):e162547.
63. Galor A, Britten-Jones AC, Feng Y, et al. TFOS lifestyle: impact of lifestyle challenges on the ocular surface. *Ocul Surf*. 2023;28:262–303.
64. Wang C, Peng Y, Pan S, Li L. Effect of insulin-like growth factor-1 on corneal surface ultrastructure and nerve regeneration of rabbit eyes after laser in situ keratomileusis. *Neurosci Lett*. 2014;558:169–174.
65. Cortina MS, He J, Li N, Bazan NG, Bazan HE. Recovery of corneal sensitivity, calcitonin gene-related peptide-positive nerves, and increased wound healing induced by pigment epithelial-derived factor plus docosahexaenoic acid after experimental surgery. *Arch Ophthalmol*. 2012;130:76–83.
66. Stepp MA, Tadvalkar G, Hakh R, Pal-Ghosh S. Corneal epithelial cells function as surrogate Schwann cells for their sensory nerves. *Glia*. 2017;65:851–863.
67. Bereiter DA, Rahman M, Thompson R, Stephenson P, Saito H. TRPV1 and TRPM8 channels and nocifensive behavior in a rat model for dry eye. *Invest Ophthalmol Vis Sci*. 2018;59:3739–3746.
68. Gupta AS, Linaburg TJ, Iacobucci E, et al. Varenicline solution nasal spray for the treatment of dry eye disease in Sjogren's disease: a pilot study. *Clin Ophthalmol*. 2025;19:1073–1084.
69. de Paiva CS, St Leger AJ, Caspi RR. Mucosal immunology of the ocular surface. *Mucosal Immunol*. 2022;15:1143–1157.
70. Ouyang W, Wu Y, Lin X, et al. Role of CD4+ T helper cells in the development of BAC-induced dry eye syndrome in mice. *Invest Ophthalmol Vis Sci*. 2021;62:25.
71. Chen Y, Chauhan SK, Lee HS, Saban DR, Dana R. Chronic dry eye disease is principally mediated by effector memory Th17 cells. *Mucosal Immunol*. 2014;7:38–45.
72. Mashimo M, Komori M, Matsui YY, et al. Distinct roles of α7 nAChRs in antigen-presenting cells and CD4(+) T cells in the regulation of T cell differentiation. *Front Immunol*. 2019;10:1102.